Macromolecules

COMMUNICATION TO THE EDITOR

pubs.acs.org/Macromolecules

Self-Assembly of Janus Composite Droplets at the Interface in Quaternary Immiscible Polymer Blends

Nick Virgilio and Basil D. Favis*

Centre de Recherche en Plasturgie et Composites (CREPEC), Department of Chemical Engineering, École Polytechnique de Montréal, Montréal, Québec, H3C 3A7, Canada

1. INTRODUCTION

Controlled synthesis and fabrication of complex microstructured materials is a common objective of several fields of materials science. In recent years, there has been a significant research effort in the controlled synthesis of anisotropic and/or patchy colloidal particles.[1−11] Their directional interactions can give rise to unique assemblies, while their heterogeneous surface chemistries can potentially enhance their interfacial activity and be exploited as useful emulsifying and catalysis agents.[12−19] As an example, a spectacular variety of such complex objects was reported by Fialkowski et al.,[20] who synthesized polymeric microspheres displaying a wide array of surface patterns by carefully balancing interfacial, buoyancy and gravitational forces between various phases, and by controlled curing of the materials. Still, some of the main challenges remain the mass production of these anisotropic objects with precise control of their shape and surface properties and chemistries. Consequently, the possibility of generating these particles within the desired material in a one-batch process could be an interesting thread of investigation.

Janus particles, a class of colloidal particles comprised of two surface regions with different chemical compositions,[21,22] are a typical type of such asymmetric colloids. While a variety of these particles have been described and experimentally synthesized in the past and recent years (among these cylinders, disks, micelles, etc.), the prototypical example is a sphere with one polar (hydrophilic) hemisphere and a second apolar one (hydrophobic) combined together to form a potentially amphiphilic particle.[23,24] These objects can be strongly anchored and interfacially active at an oil/water interface,[23−25] and their conformation at an interface has been studied theoretically by Casagrande et al.[24] and Ondarçuhu et al.[23] The main factors influencing the equilibrium position of a Janus particle at an interface are the interfacial tensions between the phases and particle, and its surface compositions and patterns. Pushing these ideas further, Binks and Lumsdon have introduced the notion of a Janus balance,[25] a concept subsequently refined by Jiang and Granick.[26] Figure 1 illustrates the three typical conformations a Janus particle can adopt at an interface following the precedent theoretical analysis.

If the particle behaves like an amphiphilic object, the hydrophilic hemisphere should be in contact with the water phase, the hydrophobic hemisphere with the oil phase and a four-phase line of contact should be observed, as the left particle in Figure 1 illustrates. However, a Janus particle could be interfacially active without displaying an amphiphilic behavior (Figure 1, center and right particles).[23] In these cases, the Janus object behaves like a particle of homogeneous surface composition and two three-phase lines of contact will be observed. Finally, it could display no interfacial activity at all and selectively locate in one specific phase (not illustrated). As a result, the concepts of surface heterogeneity, interfacial activity and amphiphilicity should be clearly distinguished when describing the behavior of colloidal particles at an interface.

In the emulsions and latex fields of research, it has been recognized for quite some time now that control of the interfacial properties yields a significant organization of the synthesized particles. In the early 70s, Torza and Mason,[27,28] based on the pioneering works of Harkins et al.,[29,30] developed and applied a thermodynamic framework to predict the equilibrium phase behavior of ternary emulsions comprised of two immiscible minor phases in a third major one. By adequately choosing the starting materials, they were able to synthesize Janus particles and elegantly explain their formation (note that at the time, the definition of a *Janus particle* had not been coined, and the possible unique properties of their ensembles did not seem to have been fully recognized and considered). Since then, a significant comprehensive body of literature on latex science and technology has emerged and expanded, and quite exotic particles have been fabricated.[31−36] While the thermodynamics of ternary systems is fairly well understood, kinetic factors can also strongly contribute to the microstructure development and are at the moment an active field of research.

The spreading coefficients, the key concepts introduced by Harkins and later refined by Torza and Mason, are used to predict the equilibrium morphology in blends and emulsions of three immiscible liquids. Typically, four types of microstructures can develop, each characterized by a set of three spreading coefficients: three morphologies are complete wetting types of systems, for which one spreading coefficient out of three is positive, while the fourth microstructure corresponds to partial wetting, with all three spreading coefficients being negative. In a ternary blend comprised of two minor phases A and C and one major phase B, two of the four possible morphologies are illustrated in Figure 2.

One important distinction between the two situations depicted in Figure 2 concerns the symmetry level of the particles. Ternary systems comprised of one major and two minor phases in which complete wetting is observed will form centrosymmetric (spherical symmetry) particles, as Figure 2a illustrates, or separate dispersions. Henceforth, Janus objects cannot be obtained from these types of systems when the microstruc-

Received: March 21, 2011
Revised: June 8, 2011
Published: July 15, 2011

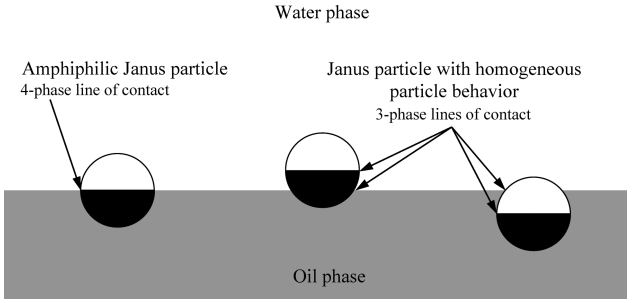

Figure 1. Schematic of interfacially active Janus particles.[23−26] Left: interfacially active and amphiphilic Janus particles. The white, hydrophilic hemisphere is in contact with water, while the black, hydrophobic hemisphere is in contact with the oil phase; Center and right: interfacially active BUT nonamphiphilic Janus particles preferring respectively the water and the oil phases. Note also the formation of a four-phase line of contact for the amphiphilic particle on the left, while two three-phase lines of contact are observed for the nonamphiphilic particles (center and right).

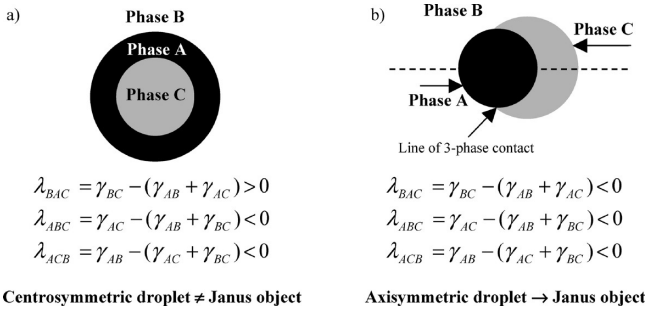

Figure 2. Two possible morphologies in a ternary immiscible system comprised of two minor phases A and C (in black and gray) and one major phase B (white), as predicted by the signs of the spreading coefficients.[27] (a) Morphology displaying complete wetting, in which the BC interface is completely wetted by phase A (note the corresponding positive spreading coefficient). The result is a particle with spherical symmetry that does not possess the attributes of a Janus object. (b) Morphology exhibiting partial wetting, in which none of the phases locates between the other two, resulting in a three-phase line of contact. The resulting droplet is axisymmetric (the axis is illustrated as the dashed line), but not centrosymmetric. As a result, this droplet possesses the attributes of a Janus object.

ture has reached equilibrium. However, at equilibrium, partial wetting yields particles that only possess cylindrical symmetry (axisymmetry, Figure 2b). This occurs when all three spreading coefficients are negative.[27] These objects are comprised of two distinct surface chemistries (A and C) that satisfy the definition of a Janus object.

In the melt-processed polymer blends field, detailed experimental works on systems displaying partial wetting were fairly scarce until recently.[37−43] While Janus particles have been observed, there appears to be no systematic study addressing their formation, potential interfacial activity and/or amphiphilic behavior in these systems, and hierarchical assembly into more complex microstructures. In a recent article, Walther et al.[44] have synthesized PS/PMMA Janus micelle particles by cross-linking a polystyrene-*block*-polybutadiene-*block*-poly(methyl methacrylate) (PS-*b*-PB-*b*-PMMA) triblock copolymer. They have shown that these micelles do segregate at

Table 1. Material Characteristics

polymers	$M_n \times 10^{-3}$ [a] (g/mol)	melt index[a] (g/10 min) (ASTM)	$\eta^* \times 10^{-3}$ (Pa·s) at 200 °C and 25 s^{-1}	$\eta_0 \times 10^{-3}$ (Pa·s) at 200 °C
HDPE	-	8.1	0.42	1.1
PP	89	35.0	0.27	0.71
PS	95 (M_w)	14.0	0.49	4.04
PMMA[b]	7.8	-	-	-
PE-*b*-PMMA	21.0-*b*-24.0	-	-	-

[a] Obtained from suppliers. [b] References 45 and 46. M_n determined by GPC.

interfaces and stabilize the microstructure when they are added to melt-processed binary blends of PS and PMMA homopolymers. However, virtually no work has investigated so far on the possibility of generating viscoelastic Janus particles directly within a melt-processed system in a one-batch process.

This article is an exploratory study that concerns morphology development in model quaternary homopolymer blend systems comprised of two major phases of high-density polyethylene (HDPE) and polypropylene (PP), and two minor phases of polystyrene (PS) and poly(methyl methacrylate) (PMMA). It specifically addresses the *in situ* formation, self-assembly, interfacial activity and amphiphilic behavior of PS/PMMA viscoelastic Janus droplets at the HDPE/PP interface. The effect of an interfacial modifier using a PE-*b*-PMMA diblock copolymer is investigated, and the results are interpreted via classical capillary and spreading coefficient theories.

2. EXPERIMENTAL METHODS

2.1. Materials. Four homopolymers and one diblock copolymer were used. A barefoot resin of high-density polyethylene, HDPE 3000, was supplied by Petromont. Polypropylene PP PD702 was obtained from Basell and polystyrene PS 615APR from Americas Styrenics. Poly(methyl methacrylate) 200336 (PMMA) was supplied by Aldrich. Finally, a diblock copolymer of 1,4-hydrogenated (ethylene-butylene)-*block*-methyl methacrylate (PE-*b*-PMMA) was synthesized by Polymer Source, Inc. The materials characteristics are listed in Table 1, and the interfacial tensions measured by a combination of the breaking thread method, Neumann triangle method and the FIB-AFM technique (NT-FIB-AFM method)[42] are given in Table 2. In all cases, the values are comparable to other results reported in the literature.[45−47]

2.2. Blend Preparation and Annealing. The HDPE/PP/PS/PMMA quaternary blends were prepared in a Plasti-Corder Digi-System internal mixer from C.W. Brabender Instruments Inc. at 200 °C and 50 rpm for 8 min under a constant nitrogen flow, with constant homopolymer volume fractions of HDPE/PP/PS/PMMA 45/45/5/5 vol. %. For the copolymer, 2 g of PE-*b*-PMMA/100 mL of PMMA (2% PE-*b*-PMMA) were added to one of the quaternary blends to modify the HDPE/PMMA interface. Quiescent annealing of the blends was then performed under a hot press at 200 °C for 30 min, after which the blends were plunged into cold water to freeze-in the morphology.

2.3. Scanning Electron Microscope Observations. Samples were initially cryogenically microtomed using a Leica

Table 2. Interfacial Tensions Obtained by the Combined Neumann Triangle and FIB−AFM Methods and Spreading Coefficients

polymer pairs	no. of measurements, N	interfacial tensions γ (mN/m)
PS/HDPE	34	4.2 ± 0.6
PS/PP	34	3.5 ± 0.2
PP/HDPE	34	1.1 ± 0.6
PMMA/HDPE	-	8.6 ± 0.9[a]
PMMA/PP	28	5.0 ± 0.8
PMMA/PS	28	1.7 ± 1.0

Spreading Coefficients (mN/m): $\lambda_{i/k/j} = \gamma_{ij} - (\gamma_{ik} + \gamma_{jk})$

HDPE/PS/PMMA: complete wetting	PP/PS/PMMA: partial wetting
$\lambda_{HDPE/PMMA/PS} = -6.1 \pm 2.5$	$\lambda_{PP/PMMA/PS} = -3.2 \pm 2.0$
$\lambda_{HDPE/PS/PMMA} = 2.7 \pm 2.5$	$\lambda_{PP/PS/PMMA} = -0.2 \pm 2.0$
$\lambda_{PS/HDPE/PMMA} = -11.1 \pm 2.5$	$\lambda_{PS/PP/PMMA} = -6.8 \pm 2.0$
HDPE/PP/PS: partial wetting	**HDPE/PP/PMMA: complete wetting**
$\lambda_{HDPE/PS/PP} = -6.6 \pm 1.4$	$\lambda_{HDPE/PMMA/PP} = -12.5 \pm 2.3$
$\lambda_{HDPE/PP/PS} = -0.4 \pm 1.4$	$\lambda_{HDPE/PP/PMMA} = 2.5 \pm 2.3$
$\lambda_{PP/HDPE/PS} = -1.8 \pm 1.4$	$\lambda_{PMMA/HDPE/PP} = -4.7 \pm 2.3$

[a] Value taken from refs. [42,46]

RM2165 microtome equipped with a LN21 cooling system. For SEM observations, the PMMA phase was subsequently extracted at room temperature for 3 days using acetic acid and then dried at 60 °C under vacuum in an oven. The samples were then coated with a gold−palladium layer by plasma sputtering. SEM observations were conducted using a JEOL JSM 840 scanning electron microscope operated at 10 kV and 6×10^{-11} A.

2.4. FIB−AFM Morphology Analysis. The combination of focused ion beam (FIB) and AFM has been shown in previous articles[42,48] to result in an excellent contrast between the phases for morphology analysis. Samples for the focused ion beam (FIB) preparation were first cryogenically microtomed. A gold−palladium layer was then deposited on the samples by plasma sputtering and, finally, the surface of the specimens was prepared with the focused ion beam. The FIB surface etching was performed using a Hitachi 2000A Ga^+ focused ion beam operated at 30 keV and 3 nA, with an etching window of 120 $\times$ 10 μm^2 and a dwelling time of 3 μs. The etched surface was then analyzed with an AFM in tapping mode using a Dimension 3100 scanning probe microscope from Veeco Instruments equipped with a Nanoscope IVa control module. Tips model PPP-NCH-W from Nanosensors, with a resonance frequency of 204−497 kHz, a force constant of 10−130 N/m, length and width of 125 $\pm$ 10 μm and 30 $\pm$ 7.5 μm, tip height of 10−15 μm and radius <10 nm were used. Topographic (height) images were subsequently treated with the AFM software to remove the effects caused by inclination of the samples and the curtain effect produced by FIB surface preparation. More details about this procedure are available in ref 48.

3. RESULTS AND DISCUSSION

3.1. Microstructure of the Quaternary System without Copolymer. After melt-processing and quiescent annealing,

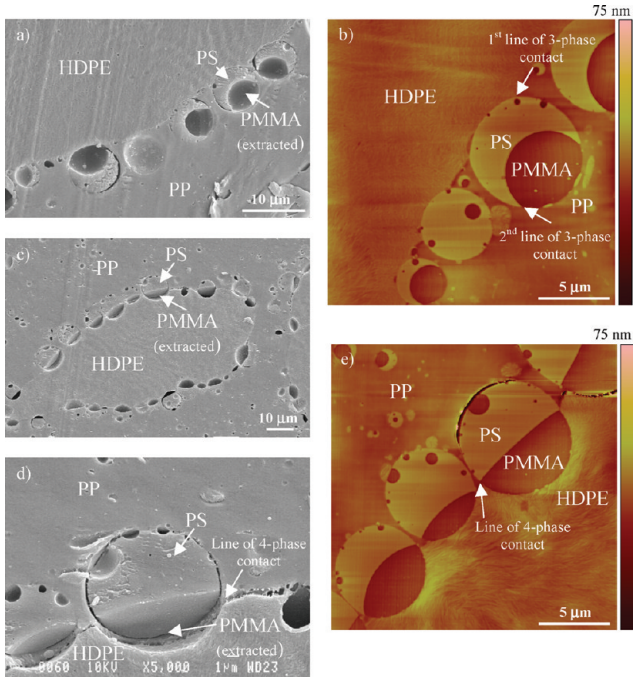

Figure 3. SEM micrograph (a) and a FIB-AFM image (b) of the unmodified HDPE/PP/PS/PMMA 45/45/5/5 blend after 30 min of quiescent annealing. Asymmetric, composite Janus PS/PMMA droplets are observed at the HDPE/PP interface, but they do not display an amphiphilic behavior. Furthermore, two three-phase lines of contact are observed. (c−e) The quaternary blend is examined, but modified this time with 2% PE-*b*-PMMA (based on the PMMA content) and annealed for 30 min. In this latter case, the PS/PMMA composite droplets have a Janus structure and also display an amphiphilic behavior, with the PS adjacent to the PP phase and the PMMA to the HDPE phase. Note finally the formation of the four-phase line of contact.

the analysis of Figure 3a,b reveals the formation of axisymmetric PS/PMMA droplets located at the HDPE/PP interfaces. This axisymmetry satisfies the definition of a Janus object and, at 50/50 PS/PMMA compositions within the droplets, the PS covers a higher fraction of a droplet's surface. However, even if they are located at the HDPE/PP interfaces, these particles do not display an amphiphilic behavior. The PS is in contact with both the HDPE and PP phases (which it prefers), while the PMMA is only in contact with the PP phase but not the HDPE. As a result, two three-phase lines of contact are observed and the Janus particles behave like homogeneous particles (see the center and right particles in Figure 1).

In trying to understand why an amphiphilic behavior is not observed, it is useful to investigate on the expected equilibrium microstructure of this unmodified quaternary HDPE/PP/PS/PMMA 45/45/5/5 blend (which has been discussed previously in a recent article[42]). For a quaternary system, as opposed to a ternary one, one set of three spreading coefficients is not enough to predict the resulting microstructure. However, the spreading coefficients of the four different ternary combinations can be analyzed (Table 2). In a ternary HDPE/PS/PMMA blend, complete wetting is theoretically predicted and experimentally observed, with the PS spreading and forming a continuous layer at the HDPE/PMMA interface.[45−48] Note that $\lambda_{HDPE/PS/PMMA} = 2.7 \pm 2.5$ is positive. The PMMA is then completely separated from the HDPE. The spreading coefficients for the PP/PS/

PMMA blend (all negative) predict a partial wetting type of morphology.[42] As a result, the minor phases of PS and PMMA dispersed in PP give composite droplets of PS and PMMA, but with the two minor phases in contact with each other and with the PP phase along a common line of contact, as the schematic of Figure 2b also illustrates. The result is similar for the HDPE/PP/PS combination, and the PS is in contact with both the HDPE and the PP phases.[41] Finally, for the HDPE/PP/PMMA ternary system, $\lambda_{HDPE/PP/PMMA}$ is positive. The PMMA is then completely separated from the HDPE by the PP phase (unpublished results). The FIB-AFM image of Figure 3b shows that all of these tendencies are respected for the studied unmodified quaternary blend, and the four sets of spreading coefficients are in agreement with the observed morphology.

The spreading coefficients analysis simply demonstrates quantitatively that the PS/PMMA Janus composite droplets do not display an amphiphilic behavior because both the PS and PMMA phases have a preferential affinity with the PP phase. To obtain both a Janus droplet type of structure and an amphiphilic character, it appears natural that one of the droplet's phase should in fact have a stronger affinity with the HDPE. This is explored in the next section.

3.2. Modified Quaternary System and Formation of Amphiphilic PS/PMMA Janus Droplets at the HDPE/PP Interface. A significant morphological transition is observed when a small amount of a PE-*b*-PMMA diblock copolymer (2% wt. based on the PMMA content) is added to the quaternary HDPE/PP/PS/PMMA 45/45/5/5 vol. % blend (Figure 3c–e, PS/PMMA volume ratio of 1:1). The PMMA migrates from the PP phase toward the HDPE phase and confirms the activity of the copolymer at the HDPE/PMMA interface. The PMMA also tends to remain in contact with the PS phase since the corresponding interfacial tension is relatively low (Table 2). As a result, PS/PMMA composite droplets displaying a side-by-side morphology are formed, with the PS hemisphere in contact with the PP and the PMMA hemisphere in contact with the HDPE. As in the previous section, these PS/PMMA composite droplets are axisymmetric with a Janus character. However, they also possess a clear amphiphilic behavior: the PS hemisphere is exclusively in contact with the PP, and the PMMA is only in contact with the HDPE. This feature is absent in the unmodified system. Furthermore, these PS/PMMA Janus droplets form a very dense array at the HDPE/PP interface, as shown in Figure 3, parts c and e.

Another significant feature is the formation of what appears to be a four-phase line of contact, which is predicted to exist theoretically,[49−51] but, to our knowledge, have not been reported until now in multiphase polymer blends. In Figure 3e, this line appears as a point and can be observed for each droplet. Figure 3d is a SEM close-up on a PS/PMMA droplet after the selective extraction of the PMMA phase, revealing where the homopolymers meet at the four-phase line. Parts a and b of Figure 4 show complementary SEM views after the selective extraction of the PS phase, with the quite visible interfaces and the four-phase lines (marked respectively with dotted red lines and black and white dots in Figure 4b). Furthermore, a similar amphiphilic behavior is observed for 75/25 PS/PMMA %vol. asymmetric droplets (PS/PMMA volume ratio of 3:1) modified with 2% PE-*b*-PMMA copolymer, as parts c and d of Figure 4 illustrate.

The transition from nonamphiphilic to amphilic droplet behavior after the addition of the PE-*b*-PMMA block copolymer is related to the minimization of the system's free interfacial energy. Ondarçuhu et al.[23] have conceptually illustrated the

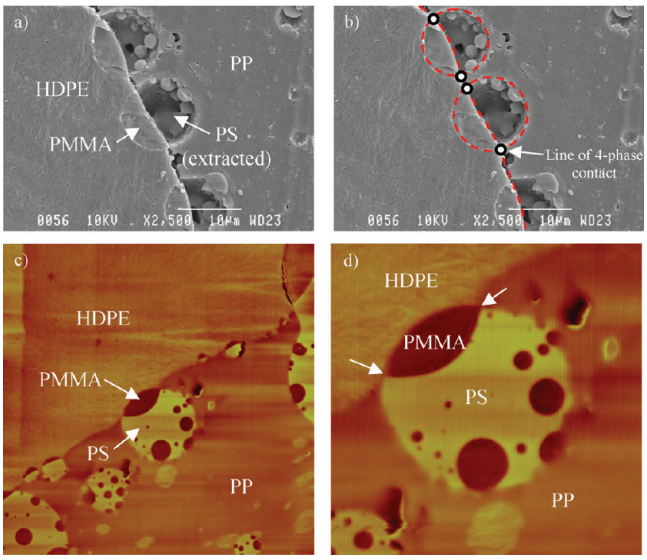

Figure 4. (a and b) SEM micrographs of the HDPE/PP/PS/PMMA 45/45/5/5 vol. % blend compatibilized with 2% PE-*b*-PMMA where the PS phase as been selectively extracted with cyclohexane (as opposed to the PMMA extraction shown in Figure 3, parts c and d). The four homopolymers meet along a common four-phase line identified with black and white dots in part b (the red dotted lines mark the different interfaces). (c and d) amphiphilic PS/PMMA Janus droplets at the HDPE/PP interface in a HDPE/PP/PS/PMMA 45/45/7.5/2.5 vol. % blend modified with 2% PE-*b*-PMMA (the PS/PMMA ratio is 3:1 instead of 1:1 as in Figure 3 and parts a and b here). An amphiphilic behavior is again observed.

activity and possible conformations of asymmetric Janus solid spherical particles at an oil/water interface. Their free energy landscape depends not only on the magnitude of the interfacial tensions, but also on the surface pattern of the particles, i.e., their surface geometry. Of the three possible conformations illustrated in Figure 1, the particles will preferentially adopt the one minimizing the free energy. The appearance of a four-phase line of contact is associated with an amphiphilic behavior and pinning of the particles at the line which separates the two different surface chemistries, as illustrated in Figure 1a.

As opposed to solid particles, viscoelastic PS/PMMA droplets can clearly deform at the interface due to the interfacial tensions. However, the physics related to their conformation should be similar, i.e., minimization of the interfacial free energy. The formation of the four-phase line between the HDPE, PP, PS, and PMMA phases can then be understood as follow: the compatibilization of the HDPE/PMMA interface with the PE-*b*-PMMA diblock copolymer strongly drives the PMMA hemisphere toward the HDPE phase, while the PS hemisphere still prefers the PP phase. As a result, the droplets are pinned at the HDPE/PP interface exactly where the PS and PMMA hemispheres meet and a four-phase line is formed. This is the conformation that minimizes the free energy of the system.

As a consequence, an important question concerns the equilibrium values of the contact angles at a four-phase line of contact in systems comprised of four immiscible liquid phases. In immiscible ternary systems displaying a three-phase line, it is well-known that contact angles are uniquely defined by balancing the three interfacial tension values in the plane perpendicular to the three-phase line[27]—this is the classical Neumann triangle

relation. There are two independent angles (the third is 360° minus the other two) and two independent spatial directions in the plane (X and Y), yielding a unique set of three contact angles for a given set of three interfacial tensions. For a four-phase line system with an equivalent number of interfacial tensions, balancing the tensions in the plane perpendicular to the line does yield multiple solutions since there are three independent angles (the fourth is 360° minus the other three) but only two independent directions (X and Y)—there are two equations with three independent parameters. To solve this problem, preliminary theoretical calculations performed in our group suggest that a unique set of contact angles is found when the relative compositions of the phases are also taken into account—supporting the theoretical existence of multiphase lines of contact. However, to our knowledge, no such theoretical treatment is available at the moment in the literature.

It is relevant to keep in mind that brief depinning of the particles could occur due to the dynamic (although relatively slow) nature of the coalescence and coarsening processes during quiescent annealing, and due to potential interactions between neighboring droplets. Furthermore, artifacts could appear due to small volumetric variations of the phases during cooling of the samples and due the microtoming procedure. These might account for the ambiguous position observed for some particles at the interface.

3.3. Neumann Triangle Method to Measure the Modified HDPE/PMMA Interfacial Tension. The Neumann equation analysis combined with the FIB−AFM technique (NT−FIB−AFM method) was used in order to measure the HDPE/PMMA modified interfacial tension.[42] Since a four-phase line of contact is formed, the classical Neumann equation needs to be modified in order to account for this new morphological feature.[49−52] Following the geometric construction depicted in Figure 5 and setting the XY reference axis at the four-phase line of contact, with the X-axis tangent to the particle's surface, the mechanical equilibrium condition along the line in the X direction is given by:

$$\gamma_{PP/PS} + \gamma_{HDPE/PP}\cos\theta_2 - \gamma_{PS/PMMA}\cos\theta_1 = \gamma_{HDPE/PMMA} \quad (1)$$

Using the interfacial tensions in Table 2, the analysis of five droplets yields an average value of 3.9 ± 1.4 mN/m (five particles analyzed) for the modified $\gamma_{HDPE/PMMA}$ interfacial tension. This represents a significant drop from 8.6 ± 0.9 to 4.7 ± 2.3 mN/m, and an apparent areal density of 0.30 ± 0.07 copolymer molecule/nm^2 is estimated for the PE-*b*-PMMA block copolymer at the HDPE/PMMA interface.[42,43]

It is pertinent to remark that although the interfacial tension decreases significantly, it does not appear to completely drop to zero, even though the HDPE/PMMA interface seems saturated in copolymer.[42,43] As pointed out in some articles,[49,53] this could be due to the elasticity of the modified HDPE/PMMA interface, a phenomena that should possibly have to be taken into account when using the Neumann method for such situations.

Another intriguing feature is the near-perfect spherical shape of the PS/PMMA amphiphilic droplets (Figures 3c−e, 4, and 5). In classical systems displaying three-phase lines of contact (such as the HDPE/PP/PS or PP/PS/PMMA lines in Figure 3, parts a and b),[27,42] a droplet's spherical shape is perturbed at the three-phase line due to the forces exerted on it by the interfacial tensions. However, this perturbation is almost imperceptible for

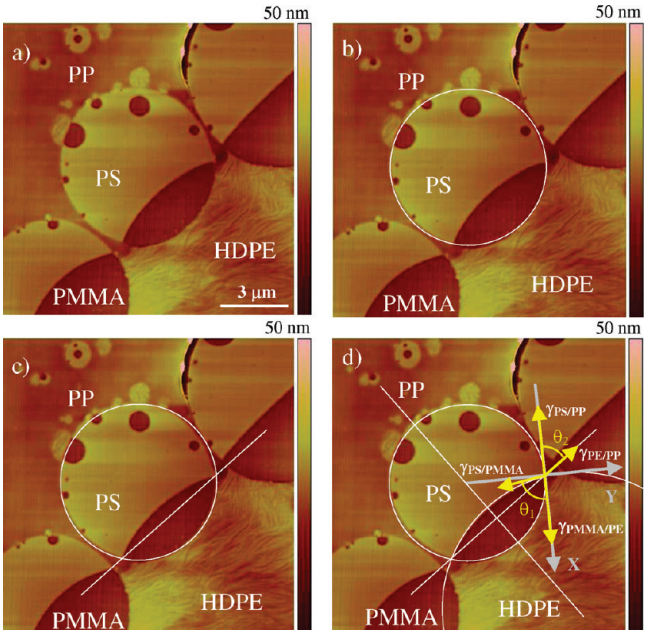

Figure 5. Application of the NT−FIB−AFM method to measure the modified $\gamma_{HDPE/PMMA}$ interfacial tension. (a to d) Demonstration of the geometric construction used to measure the modified tension.

the PS/PMMA amphiphilic droplets reported in this article. This can be explained by analyzing the interfacial tensions and geometry at the four-phase line. The PS/PMMA interfacial tension ($\gamma_{PS/PMMA}$ = 1.7 ± 1.0 mN/m, see Table 2) pulls inward the droplet and will tend to contract it at the four-phase line. However, $\gamma_{HDPE/PP}$ (=1.1 ± 0.6 mN/m, similar in magnitude to $\gamma_{PS/PMMA}$) pulls outward and almost in the opposite direction to $\gamma_{PS/PMMA}$, canceling the effect of the latter. As a result, the PS/PMMA droplets remain quasi-spherical.

A number of quaternary structures and morphological features cannot be predicted to occur by classical spreading theory, including the formation of a four-phase line of contact. Since the number of possible microstructures increases rapidly with the number of components in a blend, the usual approaches used for predicting the morphologies in multiphase systems become limited. More investigations are currently in progress to study the formation conditions and the stability of such structures in quaternary systems.

The solid state properties at ambient temperature of melt-processed polymer blends offer unique possibilities for observing and quantifying by high-resolution microscopic analysis methods the amphiphilic character and behavior of interfacially active particles. Such an analysis would prove much more difficult to conduct with classical water/oil interfaces due to their highly dynamic nature at ambient temperature. The microstructure reported in this article could prove useful for fabricating and for investigating on Janus droplets behavior.

4. CONCLUSION

Axisymmetric Janus composite droplets comprised of PS and PMMA hemispheres have been generated by melt processing unmodified and interfacially modified quaternary HDPE/PP/PS/PMMA 45/45/5/5 blends. The formation of the microstructures results from the combination of partial and complete

wetting regimes occurring between the different phases. To our knowledge, this is the first study dedicated to Janus droplets formation, interfacial activity and assembly in melt-processed polymer blends.

In the unmodified blend, Janus droplets comprised of PS and PMMA hemispheres are interfacially active and locate at the HDPE/PP interface. While the PS hemisphere is in contact with all other three phases, the PMMA is only in contact with the PP and PS. As a result, these particles possess a Janus-like architecture but behave like homogeneous particles due to the stronger affinity of the PS and PMMA phases for the PP. The addition of a PE-*b*-PMMA diblock copolymer significantly alters the microstructure. The PS/PMMA particles retain their Janus architecture, are interfacially active at the HDPE/PP interface and are still comprised of two adjacent PS and PMMA hemispheres. However, as opposed to the unmodified scenario, the PMMA hemisphere is exclusively located in the HDPE phase due to the interfacial activity of the block copolymer, while the PS is only in contact with the PP phase. As a result, these PS/PMMA particles also possess an amphiphilic behavior characterized by the formation of a four-phase line of contact. To our knowledge, this detailed experimental observation of a four-phase line of contact is the first time ever reported for a multiphase polymer blend system. Using the Neumann triangle method combined with the FIB-AFM microscopy technique, the HDPE/PMMA interfacial tension decreases from 8.6 to 3.9 mN/m as the copolymer is added, for an apparent areal density of 0.30 ± 0.07 copolymer molecule/nm^2, a value close to reported saturation values. More investigations are currently in progress to understand and predict how such complex morphologies can develop in multiphase systems.

AUTHOR INFORMATION

Corresponding Author

*E-mail: basil.favis@polymtl.ca. Telephone: +1 514 340-4711 ext. 4527. Fax: +1 514 340-4159.

ACKNOWLEDGMENT

The authors gratefully acknowledge the financial support received from the Natural Sciences and Engineering Research Council of Canada (NSERC). The authors also thank Professor Gilles L'Espérance from the Center for the Characterization and Microscopy of Materials (CM)^2 for the use of the focused ion beam and Professor Patrick Desjardins from the Department of Engineering Physics for the use of the atomic force microscope. N.V. would like to thank the Fonds Québécois de la Recherche sur la Nature et les Technologies (FQRNT) for a scholarship and Dr. Pierre Sarazin for fruitful discussions.

REFERENCES

(1) Pawar, A. B.; Kretzschmar, I. *Macromol. Rapid Commun.* **2010**, *31*, 150–168.
(2) Yuet, K. P.; Hwang, D. K.; Haghgooie, R.; Doyle, P. S. *Langmuir* **2010**, *26*, 4281–4287.
(3) Wurm, F.; Kilbinger, A. F. M. *Angew. Chem., Int. Ed.* **2009**, *48*, 8412–8421.
(4) Dendukuri, D.; Doyle, P. S. *Adv. Mater.* **2009**, *21*, 4071–4086.
(5) Walther, A.; Müller, A. H. E. *Soft Matter* **2008**, *4*, 663–668.
(6) Glotzer, S. C.; Solomon, M. J. *Nat. Mater.* **2007**, *6*, 557–562.
(7) Van Blaaderen, A. *Nature* **2006**, *439*, 545–546.
(8) Hong, L.; Jiang, S.; Granick, S. *Langmuir* **2006**, *22*, 9495–9499.
(9) Perro, A.; Reculusa, S.; Ravaine, S.; Bourgeat-Lami, E.; Duguet, E. *J. Mater. Chem.* **2005**, *15*, 3745–3760.
(10) Liu, Y.; Abetz, V.; Müller, A. H. E. *Macromolecules* **2003**, *36*, 7894–7898.
(11) Erhardt, R.; Böker, A.; Zetti, H.; Kaya, H.; Pyckhout-Hintzen, W.; Krausch, G.; Abetz, V.; Müller, A. H. E. *Macromolecules* **2001**, *34*, 1069–1075.
(12) Chen, Q.; Bae, S. C.; Granick, S. *Nature* **2011**, *460*, 381–385.
(13) Jiang, S.; Chen, Q.; Tripathy, M.; Luijten, E.; Schweizer, K. S.; Granick, S. *Adv. Mater.* **2010**, *22*, 1060–1071.
(14) Velev, O.; Gupta, S. *Adv. Mater.* **2009**, *21*, 1897–1905.
(15) Gangwal, S.; Cayre, O.; Velev, O. D. *Langmuir* **2008**, *24*, 13312–13320.
(16) Walther, A.; Hoffmann, M.; Müller, A. H. E. *Angew. Chem., Int. Ed.* **2008**, *47*, 711–714.
(17) Edwards, E. W.; Wang, D.; Möhwald, H. *Macromol. Chem. Phys.* **2007**, *208*, 439–445.
(18) Glaser, N.; Adams, D. J.; Böker, A.; Krausch, G. *Langmuir* **2006**, *22*, 5227–5229.
(19) Crossley, S.; Faria, J.; Shen, M.; Resasco, D. *Science* **2010**, *327*, 68–72.
(20) Fialkowski, M.; Bitner, A.; Grzybowski, B. A. *Nat. Mater.* **2005**, *4*, 93–97.
(21) De Gennes, P.-G. *Rev. Mod. Phys.* **1992**, *64*, 645–648.
(22) De Gennes, P.-G. *Angew. Chem., Int. Ed.* **1992**, *31*, 842–845.
(23) Ondarçuhu, T.; Fabre, P.; Raphaël, E.; Veyssié, M. *J. Phys. (Paris)* **1990**, *51*, 1527–1536.
(24) Casagrande, C.; Fabre, P.; Raphaël, E.; Veyssié, M. *Europhys. Lett.* **1989**, *9*, 251–255.
(25) Binks, B. P.; Fletcher, P. D. I. *Langmuir* **2001**, *17*, 4708–4710.
(26) Jiang, S.; Granick, S. *J. Chem. Phys.* **2007**, *127*, 161102-(1–4).
(27) Torza, S.; Mason, S. G. *J. Colloid Interface Sci.* **1970**, *33*, 67–83.
(28) Torza, S. *Interfacial Phenomena in Shear and Electrical Fields*. Ph. D. Thesis, McGill University: Montreal, 1969.
(29) Harkins, W. D.; Feldman, A. *J. Am. Chem. Soc.* **1922**, *44*, 2665–2685.
(30) Harkins, W. D. *J. Chem. Phys.* **1941**, *9*, 552–568.
(31) Chen, Y.-C.; Dimonie, V.; El-Aasser, M. S. *Macromolecules* **1991**, *24*, 3779–3787.
(32) Sundberg, E. J.; Sundberg, D. C. *J. Appl. Polym. Sci.* **1993**, *47*, 1277–1294.
(33) González-Ortiz, L. J.; Asua, J. M. *Macromolecules* **1995**, *28*, 3135–3145.
(34) Duda, Y.; Vázquez, F. *Langmuir* **2005**, *21*, 1096–1102.
(35) Herrera, V.; Palmillas, Z.; Pirri, R.; Reyes, Y.; Leiza, J. R.; Asua, J. M. *Macromolecules* **2010**, *43*, 1356–1363.
(36) Tang, C.; Zhang, C.; Liu, J.; Qu, X.; Li, J.; Yang, Z. *Macromolecules* **2010**, *43*, 5114–5120.
(37) Hobbs, S. Y.; Dekkers, M. E. J.; Watkins, V. H. *Polymer* **1988**, *29*, 1598–1602.
(38) Horiuchi, S.; Matchariyakul, N.; Yase, K.; Kitano, T. *Macromolecules* **1997**, *30*, 3664–3670.
(39) Debolt, M. A.; Robertson, R. E. *Polym. Eng. Sci.* **2006**, 385–396.
(40) Kim, J. K.; Jeong, W.-Y.; Son, J.-M.; Jeon, H. K. *Macromolecules* **2000**, *33*, 9161–9165.
(41) Virgilio, N.; Marc-Aurèle, C.; Favis, B. D. *Macromolecules* **2009**, *42*, 3405–3416.
(42) Virgilio, N.; Desjardins, P.; L'Espérance, G.; Favis, B. D. *Macromolecules* **2009**, *42*, 7518–7529.
(43) Virgilio, N.; Desjardins, P.; L'Espérance, G.; Favis, B. D. *Polymer* **2010**, *51*, 1472–1484.
(44) Walther, A.; Matussek, K.; Müller, A. H. E. *ACS Nano* **2008**, *2*, 1167–1178.
(45) Reignier, J.; Favis, B. D. *AIChE J.* **2003**, *49* (4), 1014–1023.
(46) Reignier, J.; Favis, B. D. *Macromolecules* **2000**, *33*, 6998–7008.
(47) Guo, H. F.; Packirisamy, S.; Gvozdic, N. V.; Meier, D. J. *Polymer* **1997**, *38*, 785–794.

(48) Virgilio, N.; Desjardins, P.; Pépin, M.-F.; L'Espérance, G.; Favis, B. D. *Macromolecules* **2005**, *38*, 2368.
(49) Li, D.; Neumann, A. W. *Adv. Colloid Interface Sci.* **1994**, *49*, 147–195.
(50) Chen, P.; Gaydos, J.; Neumann, A. W. *Langmuir* **1996**, *12*, 5956–5962.
(51) Shadnam, M.; Amirfazli, A. *Langmuir* **2003**, *19*, 4658–4665.
(52) Rowlinson, J. S.; Widom, B. in *Molecular Theory of Capillarity*; Dover Publications Inc.: Mineola, NY, 2002, 327p.
(53) Li, D.; Neumann, A. W. *Langmuir* **1993**, *9*, 50–54.